

Showcasing research from Professor Gangjian Wei's laboratory, State Key Laboratory of Isotope Geochemistry, Guangzhou Institute of Geochemistry, Chinese Academy of Sciences, Guangzhou, China.

Accurate *in situ* oxygen isotopic analysis at high resolution by secondary ion mass spectrometry shows the potential of aragonite as a reference material

*In situ* oxygen isotopic analysis of aragonite by secondary ion mass spectrometry is developed based on a new-developed aragonite reference material, and the evident matrix effect correlated with the aragonite calcium content is found in SIMS aragonite oxygen isotopic analysis. Corals, as biogenic carbonates, are used as examples for evaluating the application of the *in-situ* method, and the possible biocarbonate mineralization mechanisms (vital effects) were revealed.

As featured in:



See Miaohong He *et al.*,  
*J. Anal. At. Spectrom.*,  
2021, **36**, 1389.



Cite this: *J. Anal. At. Spectrom.*, 2021, **36**, 1389

# Accurate *in situ* oxygen isotopic analysis at high resolution by secondary ion mass spectrometry shows the potential of aragonite as a reference material†

Miaohong He,<sup>1</sup> Tianyu Chen,<sup>2</sup> Xi Liu,<sup>3</sup> Ya-Nan Yang,<sup>4</sup> Xiaoping Xia,<sup>5</sup> Qing Yang,<sup>6</sup> Pengli He,<sup>7</sup> Jian Di,<sup>8</sup> Yanqiang Zhang<sup>9</sup> and Gangjian Wei<sup>10</sup>

Oxygen isotopic analysis of aragonite by secondary ion mass spectrometry (SIMS) is of significance to reveal the high spatial resolution information correlated with microstructure which could not be achieved by conventional methods. Appropriate reference materials to calibrate instrumental mass fractionation of SIMS are vital to acquire accurate values. However, the scarcity of standards (as far as we know, there were just two in-house laboratory-based potential reference materials reported) limits the development of this field. Herein, an inorganically precipitated aragonite vein sample (VS001/1-A) being evaluated through several hundred SIMS oxygen isotopic analyses was ascertained to have homogeneous oxygen isotopic composition with an external reproducibility of 0.3‰ (1 $\sigma$ ) and to be a potential SIMS reference material. The instrumental bias evident in the series of aragonites, decreased by ~3.4‰ with decreasing aragonite Ca content. Corals, as biogenic carbonates, were used as examples for evaluating the application of the *in situ* SIMS analysis method, and processes involved in “vital effects” are described. The development of *in situ* oxygen isotopic microanalysis of aragonite is significant for the application of revealing possible biocarbonate mineralization mechanisms.

Received 1st March 2021  
 Accepted 17th May 2021

DOI: 10.1039/d1ja00072a

rsc.li/jaas

## 1. Introduction

Aragonite, one of the most abundant calcium carbonate minerals on Earth, constitutes the dominant skeletal material of many marine organisms including coral, bivalve and calcareous algae.<sup>1</sup> Oxygen isotopes in aragonite have been widely studied with well-established proxies in reconstruction of changes in climatic and palaeoceanographic conditions.<sup>2–6</sup> However, previous work has been based primarily on conventional analysis (phosphoric acid digestion and then gas-source mass spectrometry analysis) that requires time-consuming sample pretreatment and has coarse sampling resolutions (typically 0.5–1.0 mm).<sup>7,8</sup> Corals comprise complicated skeleton micro-structures including fasciculi and centers of calcification (1–10  $\mu$ m in size) with distinct oxygen isotopic compositions

that cannot be distinguished by conventional analysis, which has low spatial resolution.<sup>7,9–11</sup> Diagenetic alterations within fossil corals are very common, and typically include infilling of skeletal pore spaces with secondary cements, dissolution of primary coral aragonite, and recrystallization, which may significantly alter the initial coral oxygen isotopic composition.<sup>12–16</sup> The inability to resolve these secondary alterations with conventional analysis may lead to appreciable uncertainties in fossil coral-based paleoclimate reconstructions.<sup>12,16</sup>

Compared with conventional bulk analysis, *in situ* oxygen isotopic analysis may avoid complicated sample pretreatment,<sup>8,17</sup> and contamination derived from alteration, and may also be able to distinguish centers of calcification and fasciculi microstructures.<sup>9–11</sup> Furthermore, it is the exclusive method with potential to reconstruct climate and environments with higher resolution (weekly, daily, or diurnal) due to its higher spatial resolution (30  $\mu$ m or less) than conventional analysis.<sup>18</sup> Therefore, it is essential to further develop *in situ* oxygen isotopic analysis, and SIMS is currently the only technique with effective spatial resolution, on a scale of a few  $\mu$ m,<sup>19</sup> allowing *in situ* analysis of zonation and its correlation with textures.<sup>9,20,21</sup> However, a critical aspect limiting the development of this method is the lack of reference materials for use in correcting the complex but systematic instrumental mass fractionation (IMF) that occurs during the measurement of isotope ratios by

<sup>1</sup>State Key Laboratory of Isotope Geochemistry, Guangzhou Institute of Geochemistry, Chinese Academy of Sciences, Guangzhou 510640, China. E-mail: mhhe@gig.ac.cn; Tel: +86-20-85290501

<sup>2</sup>CAS Center for Excellence in Deep Earth Science, Guangzhou, 510640, China

<sup>3</sup>Southern Marine Science and Engineering Guangdong Laboratory, Guangzhou, 511458, China

<sup>4</sup>MOE Key Laboratory of Surficial Geochemistry, Department of Earth and Planetary Sciences, Nanjing University, Nanjing 210023, China

† Electronic supplementary information (ESI) available. See DOI: 10.1039/d1ja00072a



SIMS and can significantly affect its analytical accuracy according to the findings of Eiler *et al.*<sup>19</sup> and Fabrega *et al.*<sup>22</sup> The magnitude of IMF depends on instrumental parameters such as sample sputtering/ionization, and secondary ion transmission and detection.<sup>20,23</sup> This fractionation is partly matrix-related, due to mineral crystal structure and composition.<sup>4,19,24</sup> However, no such well distributed aragonite standards are currently available, with only a few in-house laboratory-based standards being reported, *e.g.*, Rollion-Bard *et al.*<sup>4,10,25</sup> reported an in-house aragonite reference material for which  $\delta^{18}\text{O}_{\text{V-PDB}} = -7.18 \pm 0.22\text{‰}$  ( $1\sigma$ ), where the oxygen isotopic composition is expressed in the usual per mil notation (‰) relative to the “Vienna Pee Dee Belemnite (V-PDB)” marine carbonate reference material, and Jones *et al.*<sup>21</sup> reported another standard, BB-Ar ( $\delta^{18}\text{O}_{\text{V-PDB}} = -7.79 \pm 0.25\text{‰}$  ( $1\sigma$ )). A critical aspect of the further advancement of *in situ* aragonite oxygen isotopic analysis is thus the continued development of reference materials to correct SIMS IMF. Previous studies by Fayek *et al.*<sup>26</sup> and Rollion-Bard *et al.*<sup>27</sup> about instrumental bias or matrix effects in SIMS oxygen isotopic analyses of carbonates have involved minerals such as calcite, dolomite, ankerite, rhodochrosite, magnesite, and siderite with the Mg content contributing to IMF in Fe- and Mn-poor carbonates, but the functional relationship between IMF and the matrix composition of aragonites is poorly understood.

Considering the scarcity of aragonite standards and the lack of knowledge about SIMS aragonite oxygen isotopic analysis, this study focused on developing a new natural inorganic aragonite reference material with homogenous oxygen isotopes at the micrometer scale. Other aragonite materials, including inorganic aragonites and corals, and two available calcites were used to characterize the method. Precise oxygen isotopic compositions of these mineral were also determined by a conventional method. Two coral specimens were adopted to evaluate the application of the *in situ* analytical method.

## 2. Materials and methods

### 2.1 Sample preparation

The analyzed samples included three natural inorganic aragonite crystals, VS001/1-A, Ara-1, Ara-2; two natural aragonite-based corals; and two calcites, NBS18 and Cal-1. VS001/1-A has previously been used as a U–Th dating standard material,<sup>28</sup> and was collected from the Salt Wash Graben, Green River, Utah, USA. It was formed through upward leakage through fractures of CO<sub>2</sub>-rich fluid from a fluid reservoir in the Jurassic Navajo Sandstone.<sup>29,30</sup> The other two inorganic aragonites (Ara-1 and Ara-2) and calcite (Cal-1) were purchased from a mineral fair, and the likely provenance of both aragonite is Tazouta, Sefrou Province Morocco, but the provenance of Cal-1 is unknown. NBS18 is a US Geological Survey standard. The corals were a living *Porites* species drilled underwater drilling from colony of ~2 m radius at depth of 2.5 m on Qilianyu Reef, Xisha Islands, South China Sea (Fig. 1). The chronology of the coral had been established previously.<sup>8</sup> The corals samples were sliced parallel to the axis of maximum skeletal growth over an interval corresponding to a growth period of 1999–2000. They were divided into two sections of low- and high-density skeleton, based on X-ray photography. The corals were immersed in 10% H<sub>2</sub>O<sub>2</sub> for 24 h to remove organic matter, cleaned ultrasonically at 60 kHz (360 W) in deionized water for 30 min to remove surface contaminants, dried, and mounted in epoxy resin following Zou *et al.*<sup>31</sup> All carbonates were mounted in epoxy, polished, and coated with gold.

### 2.2 Analytical procedures

**2.2.1 Crystal identification by Raman microscopy.** Mineral crystals were identified using a confocal Raman microscope (WITec Alpha-300R, Ulm, Germany) equipped with a 532 nm laser and Zeiss 50× objective at the State Key Laboratory of Isotope Geochemistry, Guangzhou Institute of Geochemistry, Chinese Academy of Science (SKLaBIG-CAS), Guangzhou,

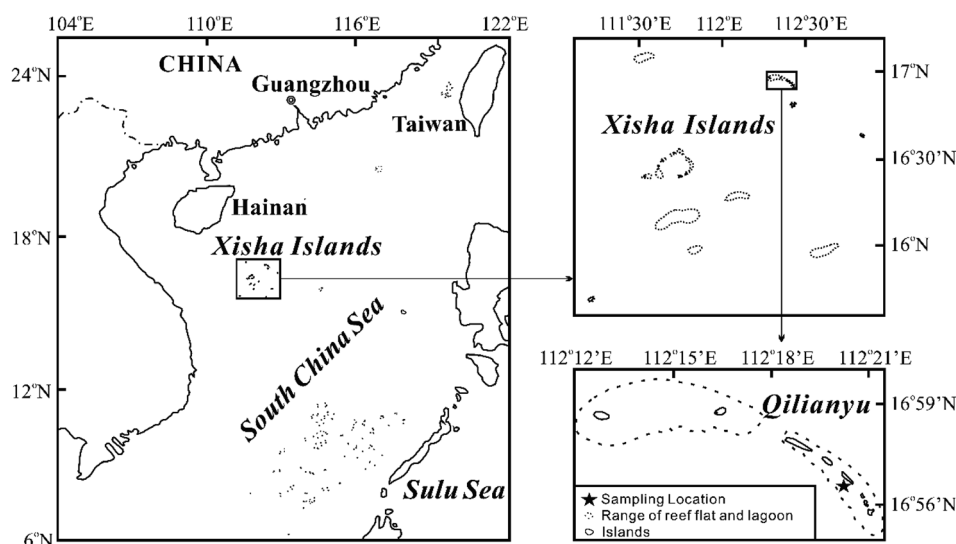


Fig. 1 Location of coral sampling for oxygen isotopic ratio analyses; from Wang *et al.*<sup>8</sup>

China. Measurements were performed at room temperature with a laser power of 30 mW, integration time of 10 s, and a wavenumber range of 80–1400  $\text{cm}^{-1}$ .

**2.2.2 Compositional analysis by EPMA.** Major and minor element compositions of minerals were determined by an electron microprobe analysis (EPMA; CAMECA SXFIVEFE, France) at the SKLaBIG-CAS with a 15 kV accelerating voltage, 20 nA beam current, and 20  $\mu\text{m}$  beam diameter. The major element Ca was separately measured with a 20 s integration time prior to the minor elements Sr, Mg, S with integration times of 120 s to avoid distortion of the Ca signal with a longer integration time. The reference materials calcite (Ca), pyrope (Mg), strontium sulfate (Sr), and pyrite (S) were used for EPMA calibration.

**2.2.3 Oxygen isotopic analysis by SIMS.** *In situ* oxygen isotopic analyses were carried out using ion microprobes (CAMECA IMS 1280-HR) at the SKLaBIG-CAS and Beijing Research Institute of Uranium Geology (BRIUG) by different operators, respectively. The primary  $\text{Cs}^+$  ion beam current had a current of  $\sim 2$  nA, diameter of  $\sim 15$   $\mu\text{m}$  and impact energy of 20 keV, with a normal-incidence electron-flood gun used for charge compensation. Each analysis was pre-sputtered for 30 s before data collection to remove the gold coating. A field aperture of  $5000 \times 5000$   $\mu\text{m}$  and contrast aperture of 400  $\mu\text{m}$  were applied. The  $^{18}\text{O}$  and  $^{16}\text{O}$  ions were collected simultaneously in two off-axis Faraday cups (L/2 and H1) with mass resolutions (full width at half maximum) of 2400. A typical secondary ion intensity for  $^{16}\text{O}$  was in the range of  $(2\text{--}3) \times 10^9$  counts per s.

Coral samples were analyzed along the fasciculi, approximately midway between the center of calcification (COC) and the trabecula, avoiding the COC with distinctly different oxygen isotopic and high organic compositions compared with the fasciculi,<sup>9,32</sup> which can be readily identified in thin section where it appears as fine dark lines or spots with diameters of 5–10  $\mu\text{m}$  at the approximate center of each skeletal structure (ESI Fig. 1†).<sup>33,34</sup> SIMS analysis spots were separated by distances of  $\sim 40$   $\mu\text{m}$  in the continuous trabecula of corals exposed within the epoxy (ESI Fig. 1†), with minor deviations to avoid COC and micro-borings. The natural aragonite crystal (VS001/1-A) was analyzed after every 5–8 coral analyses to normalize coral data. Oxygen isotopic compositions are expressed in the usual per mil notation relative to the Vienna Pee Dee Belemnite (V-PDB;  $^{18}\text{O}/^{16}\text{O}_{\text{V-PDB}} = 0.0020672$ ) which was frequently adopted as the reference for oxygen isotopic calculation instead of Vienna Standard Mean Ocean Water (VSMOW;  $^{18}\text{O}/^{16}\text{O}_{\text{VSMOW}} = 0.0020052$ ) when performing paleoenvironmental study, and IMF corrections were calculated as follows:<sup>4,35</sup>

$$\delta^{18}\text{O}_{\text{SIMS}} = ((^{18}\text{O}/^{16}\text{O}_{\text{SIMS}})/(^{18}\text{O}/^{16}\text{O}_{\text{V-PDB}}) - 1) \times 1000 \quad (1)$$

$$\text{IMF} = \delta^{18}\text{O}_{\text{SIMS}} - \delta^{18}\text{O}_{\text{actual}} \quad (2)$$

where  $^{18}\text{O}/^{16}\text{O}_{\text{SIMS}}$  is the raw ratio measured by SIMS, and  $\delta^{18}\text{O}_{\text{SIMS}}$  and  $\delta^{18}\text{O}_{\text{actual}}$  values reflect SIMS analyses and analyses by conventional technique or recommended values, respectively.

**2.2.4 Bulk  $\delta^{18}\text{O}$  analysis by phosphoric acid digestion and gas-source MS.** Oxygen isotopic compositions of VS001/1-A, Ara-1, Ara-2, and Cal-1 were determined at SKLaBIG-CAS by isotope-ratio mass spectrometry (IRMS; GV Isoprime II; Germany) with a conventional phosphoric acid digestion system. During each measurement session, powdered sample (1 mg) was digested with 102%  $\text{H}_3\text{PO}_4$  at 90  $^\circ\text{C}$  to extract  $\text{CO}_2$ . IRMS  $\delta^{18}\text{O}$  analyses of the corals had been undertaken previously by Wang *et al.*<sup>8</sup> with sampling in the same direction 5 mm away from and parallel the SIMS analytical profile, with corresponding skeletal data being compared with  $\delta^{18}\text{O}$  data from SIMS analyses. NBS19, a limestone standard from NIST with certified value for  $\delta^{18}\text{O}$  relative to V-PDB of  $-2.20\text{‰}$ <sup>36</sup> was adopted as the standard with a precision of  $\pm 0.1\text{‰}$  ( $1\sigma$ ).

## 3. Results

### 3.1 Crystal and major element composition of new reference materials

Minerals were identified by Raman analyses with results as shown in Fig. 2. Based on the distinguishing aragonite and calcite peaks at  $\sim 210$   $\text{cm}^{-1}$  and  $\sim 290$   $\text{cm}^{-1}$  (lattice mode), respectively,<sup>37,38</sup> VS001/1-A, Ara-1, and Ara-2 were identified as aragonites and Cal-1 and NBS18 as calcites.

The homogeneity of the calcium composition of these carbonates was evaluated by EPMA analysis (Table 1), with a variability of 15 measurement across 10 fragments of  $< 0.67\%$  ( $1\sigma$ ). Minor element (Sr, Mg, and S) compositions were relatively heterogeneous with variabilities of  $> 10\%$  ( $1\sigma$ ).

### 3.2 Oxygen isotopic composition of new reference materials

The oxygen isotopic compositions of VS001/1-A, Ara-1, Ara-2, and Cal-1 obtained by conventional mass spectrometry are shown in Table 2. The homogeneity of these materials was

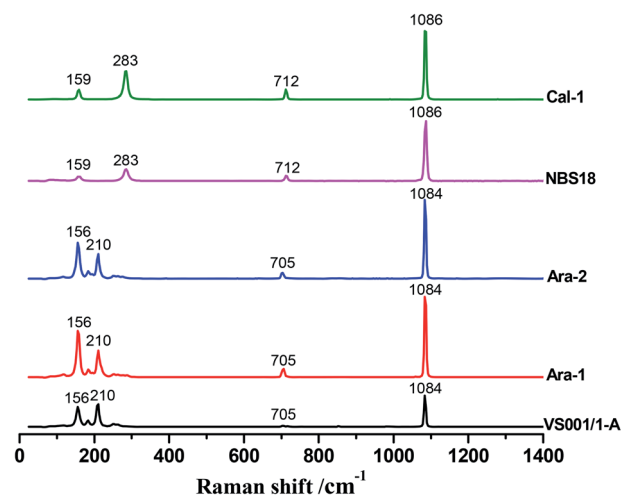


Fig. 2 Raman microscopy spectra for VS001/1-A, Ara-1, Ara-2, NBS18, and Cal-1, showing overlapping peaks in the regions of  $\sim 156$ ,  $\sim 705$  and  $\sim 1084$   $\text{cm}^{-1}$  and mineral-specific peaks of aragonite and calcite at  $210$   $\text{cm}^{-1}$  and  $283$   $\text{cm}^{-1}$ , respectively.

**Table 1** Major and minor element compositions of aragonite and calcite samples as determined by EPMA ( $n = 15$  for all samples except corals, for which  $n = \sim 140$ )<sup>a</sup>

Element	VS001/1-A		Ara-1		Ara-2		Cal-1	
	Content wt%	$2\sigma$	Content wt%	$2\sigma$	Content wt%	$2\sigma$	Content wt%	$2\sigma$
Ca	39.20	0.29	40.23	0.20	40.16	0.55	40.19	0.22
Mg	—	—	—	—	—	—	—	—
Sr	0.83	0.29	0.23	0.05	0.23	0.12	—	—
S	0.07	0.03	—	—	—	—	—	—

Element	NBS18		Low-density skeleton of coral		High-density skeleton of coral	
	Content wt%	$2\sigma$	Content wt%	$2\sigma$	Content wt%	$2\sigma$
Ca	37.71	0.65	37.98	0.53	38.10	0.56
Mg	0.36	0.19	0.06	0.03	0.06	0.03
Sr	0.70	0.18	0.77	0.04	0.78	0.05
S	—	—	0.15	0.02	0.14	0.02

<sup>a</sup> The unmeasured CO<sub>2</sub> were set to 44 wt% prior analysis, which was used to correct the matrix effect in the EPMA analysis.

determined by *in situ* SIMS analyses of different grains with random sampling over several measurement sessions in different laboratories.

Multiple bulk analyses (IRMS) of VS001/1-A in two sessions yielded a mean  $\delta^{18}\text{O}$  value of  $-12.41\text{‰} \pm 0.03\text{‰}$  ( $1\sigma$ ;  $n = 2$ ). Its homogeneity was evaluated over 140 different fragments, for

**Table 2** Summary of mean  $\delta^{18}\text{O}$  and IMF values for each sample, as determined by SIMS in different laboratories

Session	Sample	Mean $\delta^{18}\text{O}_{\text{uncorrected}}$ value determined by SIMS/‰	No.	Mean $\delta^{18}\text{O}$ value determined by conventional method/‰	IMF	SD
<b>GIG-CAS CAMECA IMS 1280-HR</b>						
20201221	1	VS001/1-A	14	$-12.41 \pm 0.03$	-0.45	0.29
		NBS18	15	$-23.06 \pm 0.26$ (ref. 39)	-0.61	0.26
		Cal-1	15	$-14.03 \pm 0.16$ (ref. 40)	-0.76	0.34
		Ara-1	15	$-7.38 \pm 0.14$	0.91	0.64
		Ara-2	15	$-6.96 \pm 0.18$	0.47	0.50
20200706	2	VS001/1-A	8		0.28	0.25
		NBS18	6		0.11	0.23
		Cal-1	11		-0.1	0.42
		Ara-1	9		1.44	0.55
		Ara-2	15		1.29	0.58
20200526	3	VS001/1-A	24		-2.47	0.31
		Ara-1	11		-1.2	0.60
		Ara-2	13		-2.04	0.50
20200526	4	VS001/1-A	19		-2.25	0.19
		Ara-1	7		-1.04	0.63
		Low density skeleton	142	$-5.75 \pm 0.14$	-4.46	0.53
20200525	5	VS001/1-A	26		-3.26	0.32
		Ara-1	14		-1.92	0.71
		High density skeleton	129	$-6.16 \pm 0.20$	-5.31	0.77
20190831	6	VS001/1-A	67		-4.21	0.27
20190830	7	VS001/1-A	51		-4.03	0.28
		Ara-1	9		-3.27	0.62
20181125	8	VS001/1-A	53		1.84	0.28
<b>BRIUG CAMECA IMS 1280-HR</b>						
20210419	9	VS001/1-A	22		-5.99	0.29
		NBS18	12		-5.92	0.2
		Cal-1	13		-6.01	0.41
		Ara-1	15		-5.15	0.29
		Ara-2	13		-5.22	0.41

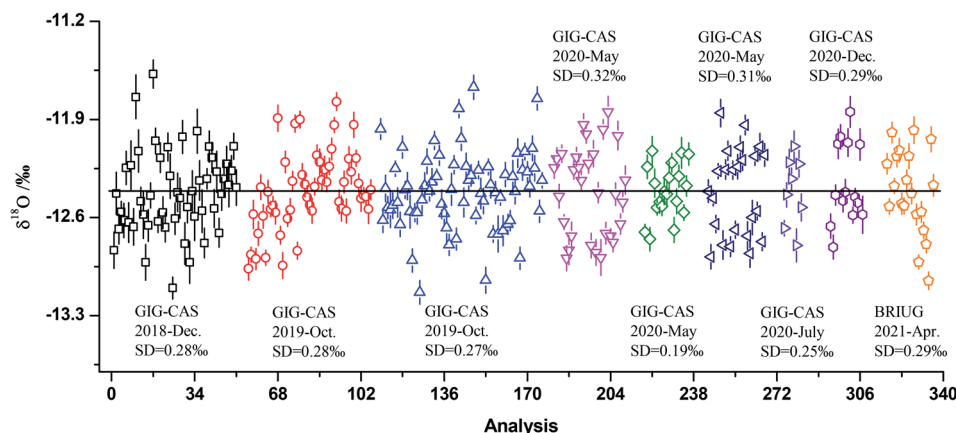


Fig. 3 Long-term reproducibility (4 years) of  $\delta^{18}\text{O}$  values (having been corrected by IMF) of different VS001/1-A fragments determined by SIMS (CAMECA IMS 1280-HR) (error bars correspond to internal precision for a single spot measurement). SD indicates the standard deviation for all measurements in each session; the horizontal line represents its true value ( $-12.41\text{‰}$ ) determined by bulk analysis. All data are corresponding to ESI Table 1.†

a total of 285 points measured  $\delta^{18}\text{O}$  in nine SIMS sessions, yielding session  $\sigma$  values of  $0.28\text{‰}$ ,  $0.28\text{‰}$ ,  $0.27\text{‰}$ ,  $0.32\text{‰}$ ,  $0.19\text{‰}$ ,  $0.31\text{‰}$ ,  $0.25\text{‰}$ ,  $0.29\text{‰}$  and  $0.29\text{‰}$  (Fig. 3 and Table 2).

Bulk-analysis means for Ara-1, and Ara-2 acquired by multiple analyses during a session were  $-7.38\text{‰} \pm 0.14\text{‰}$  ( $1\sigma$ ;  $n = 2$ ) and  $-6.96\text{‰} \pm 0.18\text{‰}$  ( $1\sigma$ ;  $n = 2$ ), respectively. They seem not significantly different from each other. Multi-point SIMS oxygen isotopic analyses over 50 fragments of each material indicate that neither is particularly homogenous, with  $\sigma$  values of up to  $\geq 0.4\text{‰}$  (Table 2). The homogeneity of calcite Cal-1 was determined over just 20 different grain fragments with a total of 39 points analyzed, with reproducibility of  $0.4\text{‰}$  ( $1\sigma$ ) and a mean bulk  $\delta^{18}\text{O}$  value of  $-14.03\text{‰} \pm 0.16\text{‰}$  (Table 2).

Furthermore, in order to evaluate the possible correlation between IMF and aragonite compositions, elemental EPMA

analyses of the aragonites were combined. The broad increase in IMF from coral to Ara-1 seems parallel the increase in Ca content of aragonite (Fig. 4), indicating that minor change in chemistry (Ca content) may have a significant effect on SIMS  $\delta^{18}\text{O}$  determinations.

### 3.3 Oxygen isotopic composition of the biogenic carbonate

SIMS oxygen isotopic analyses indicate large  $\delta^{18}\text{O}$  variation ( $\geq 4\text{‰}$ ) on a micrometer scale in the coral skeletons where low- and high-density skeleton  $\delta^{18}\text{O}$  values ranged from  $-4.68\text{‰}$  to  $-7.44\text{‰}$  and from  $-3.49\text{‰}$  to  $-8.61\text{‰}$ , respectively, which are not observed with conventional analyses (Fig. 6). This extends the total variation on a millimeter scale by  $\sim 0.33\text{‰}$  for low-density skeleton, to between  $-5.68\text{‰}$  and  $-5.81\text{‰}$ ; and by

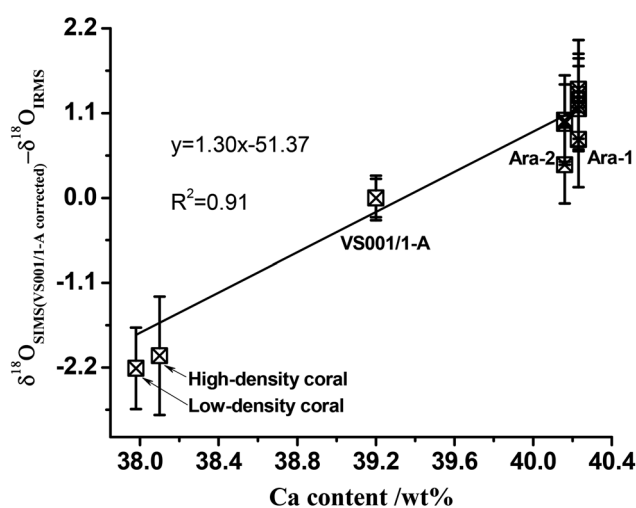


Fig. 4 Matrix effect plotted as a function of Ca content of aragonites. The matrix bias ( $\delta^{18}\text{O}_{\text{SIMS}}(\text{VS001/1-A corrected}) - \delta^{18}\text{O}_{\text{IRMS}}$ ) indicates that all samples were corrected by VS001/1-A in each session. Error bars represent external precision (or reproducibility) of multiple measurements ( $1\sigma$ ).

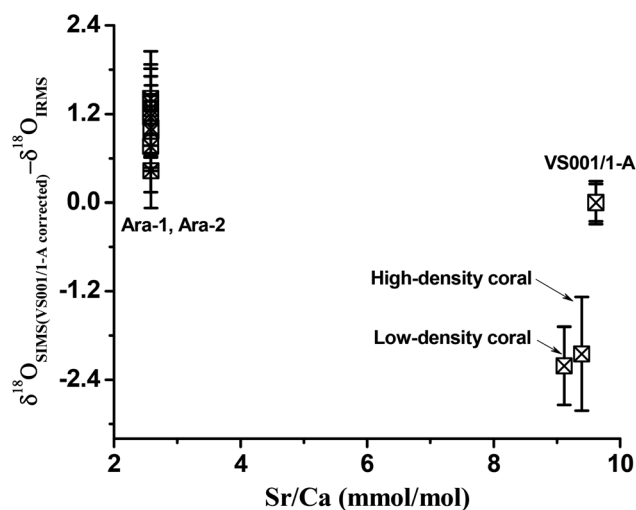


Fig. 5 Relationship between the Sr/Ca of aragonites and matrix bias. The matrix bias ( $\delta^{18}\text{O}_{\text{SIMS}}(\text{VS001/1-A corrected}) - \delta^{18}\text{O}_{\text{IRMS}}$ ) indicates that all samples were corrected by VS001/1-A in each session. Error bars represent external precision (or reproducibility) of multiple measurements ( $1\sigma$ ).

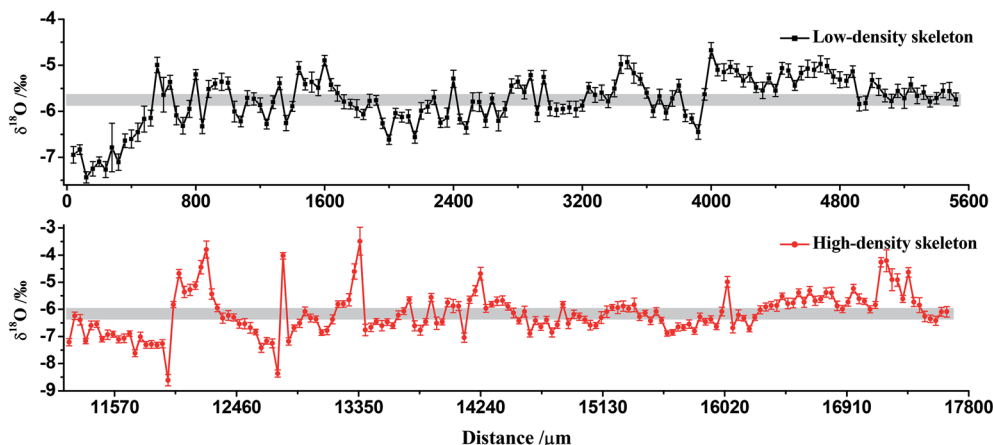


Fig. 6 SIMS  $\delta^{18}\text{O}$  values along the growth axis of coral with a spatial resolution of  $\sim 40\ \mu\text{m}$ , corresponding to low- and high-density skeletons for one year (1999–2000) of coral growth. Error bars represent the measurement precision ( $2\sigma$ ). The grey field corresponds to the range of  $\delta^{18}\text{O}$  values measured at millimeter scales by conventional method. The sample photomicrograph and SIMS analysis trajectory could be observed in ESI Fig. 1.†

$\sim 0.24\text{‰}$  for high-density skeleton, to between  $-6.27\text{‰}$  and  $-6.03\text{‰}$ .<sup>8</sup>

## 4. Discussion

### 4.1 Oxygen isotopic homogeneity of new reference materials

Fig. 3 and Table 2 indicate aragonite VS001/1-A has homogeneous  $\delta^{18}\text{O}$  composition with a mean external reproducibility of  $0.3\text{‰}$  ( $1\sigma$ ) or less, similar to that reported for other laboratory-based aragonite standards.<sup>4,21,25,41</sup> The interlaboratory comparison (Table 1) again ascertains the quality of this material. Previous work by Tang *et al.*<sup>42</sup> and Liu *et al.*<sup>43</sup> indicate that correcting the topography effect (based on the correlation between instrumental dynamic transfer parameters and measured  $\delta^{18}\text{O}$ ) could greatly improve external precision and accuracy of SIMS isotopic analysis, but it could be precluded based on the insignificant correlation between measured  $\delta^{18}\text{O}$  and instrumental dynamic transfer parameters herein (ESI Fig. 2.†). An external reproducibility of  $0.3\text{‰}$  is considered acceptable for SIMS analyses,<sup>4,24,25</sup> so VS001/1-A may be satisfactory for routine application as a reference material for SIMS isotopic microanalysis. The  $\delta^{18}\text{O}$  composition of other aragonites Ara-1 and Ara-2 are not so homogeneous as VS001/1-A.

### 4.2 IMF and matrix effects

It is common in SIMS analyses for IMF to vary between sessions, possibly due to variations in instrumental conditions from day to day. The IMF magnitude of SIMS aragonite oxygen isotopic analyses were found to vary by up to several per mil between different measurement sessions (Table 2). However, the similar bias in IRMS-determined  $\delta^{18}\text{O}$  values for each aragonite material after normalization to VS001/1-A values over different SIMS sessions (Table 2 and Fig. 4) indicates that the matrix component causes bias that is reproducible over time, within analytical uncertainty. The accurate determination of oxygen isotopic ratios thus requires calibration with standards during the same

session. Aragonite materials Ara-1, Ara-2, and two corals were used to evaluate the method of correction by VS001/1-A (assuming their IMF values are the same in SIMS analysis). Mean  $\delta^{18}\text{O}$  values of the two corals were calculated from SIMS data for  $\sim 140$  spots, with their true values expected to be within the  $\delta^{18}\text{O}$  range measured at millimeter scales.<sup>21,34,41,44</sup> However, there were significant differences between  $\delta^{18}\text{O}$  values estimated by conventional analyses and those from SIMS analyses (even with correction of all data by VS001/1-A) from one aragonite sample to the other, with a bias of up to  $3.4\text{‰}$  during a single session (Fig. 4 and Table 2). This has previously been observed with SIMS oxygen isotopic analyses of other minerals such as garnet, dolomite, calcite, and glass,<sup>20,24,27,35,45</sup> and was ascribed to physical properties including the strength of chemical bonds between the analyzed ion and its matrix,<sup>46</sup> mean atomic mass,<sup>19,24,35</sup> mole fractions of various elements (*e.g.*, Fe + Mn, Ca, Mg),<sup>27,35,45</sup> or molar volume.<sup>24,35</sup> However, the cause of the effect with aragonite is not well understood. The previous work by Allison *et al.*<sup>34</sup> had demonstrated that minor element compositions (*e.g.*, Sr/Ca ratios) could affect SIMS IMF in  $\delta^{18}\text{O}$  determination for aragonites. However, the relationship is not so obvious here for the inorganic and bio-aragonites (Fig. 5). In contrast to Sr/Ca, the Ca content herein may have a significant effect on SIMS  $\delta^{18}\text{O}$  determinations (Fig. 4). The fundamental cause may be that an impurity such as an organic phase, a minor elements effect, or substitution for Ca in the aragonite lattice may result in lattice distortion in the aragonite,<sup>47</sup> inducing a matrix effect in SIMS oxygen isotopic analysis.

The two calcites NBS18 and Cal-1, which have Ca contents approaching the maximum and minimum values for aragonites, were used to evaluate IMF between calcite and aragonite, but no differences in IMF values between them and aragonite VS001/1-A were found (Table 2). The effect of mineral crystal differences between calcite and VS001/1-A on SIMS IMF in oxygen isotopic analysis may thus be insignificant. This differs from the previous finding of Rollion-Bard *et al.*<sup>44</sup> who found



that the mean difference in IMF between calcite and aragonite was 2.8‰. That difference was attributed to the dissimilarity in bond energy between the two crystal systems.<sup>4</sup> However, IMF with VS001/1-A here was very similar to that of the two calcites in the same session (Table 2), perhaps indicating that there is an unknown factor compensating for the difference in crystallography (bond energy) and Ca content between these minerals during SIMS oxygen isotopic analysis.

These observations can be summarized as follows.

IMF in SIMS oxygen isotopic analyses under the same experimental conditions varies by up to 3.4‰ among the aragonites, with a degree of correlation with sample matrix composition (Ca contents) (Fig. 4). A significant matrix effect is thus observed in SIMS analyses of aragonites and the correlations observed with IMF could be used for empirical correction of SIMS oxygen isotopic analyses of aragonite. IMF can be satisfactorily corrected through its linear regression with Ca content, whereby a change in Ca content of 1 wt% correlates with a change in IMF of 1.3‰. This confirms that major element compositions of standards and samples must be accurately determined prior to oxygen isotopic analysis.

When an aragonite of unknown oxygen isotopic composition is analyzed, the analytical precision should take into consideration (a) the internal precision or within-spot uncertainty of the analysis, (b) uncertainty related to the reference material (*e.g.*, VS001/1-A), during the measurement session, and (c) the uncertainty of the matrix correction. Therefore, the final  $\delta^{18}\text{O}$  value of an analysis should be corrected as follows:<sup>45</sup>

$$\delta^{18}\text{O}_{\text{final}} = \delta^{18}\text{O}_{\text{SIMS}} - \text{IMF} - \text{bias} \quad (3)$$

where  $\delta^{18}\text{O}_{\text{SIMS}}$  is the raw value from SIMS analysis, IMF is the matrix-independent mass fractionation of the primary reference material (VS001/1-A), and bias is the matrix effect of a given composition.

### 4.3 Oxygen isotopic analysis of biogenic carbonate: application to corals

Biogenic carbonates often contain about 3% non-mineral components, which are mainly organic matter.<sup>48,49</sup> Nevertheless, contamination by organic matter is precluded here by the negative relationship between the  $^{16}\text{O}$  intensity and  $\delta^{18}\text{O}$  values (Fig. 7), with secondary ion ( $^{16}\text{O}$ ) intensities being  $\geq 2.4 \times 10^9$  counts per s rather than the lower count rates of  $\sim 5 \times 10^5$  counts per s for organic matter, and with  $\delta^{18}\text{O}$  values being far higher than those of coral organic matter ( $-13\text{‰}$  to  $-20\text{‰}$ ).<sup>4,50</sup> If the samples were contaminated by organic matter, the  $\delta^{18}\text{O}$  values would be positively correlated with secondary ion intensity, which is not the case here.

Coral micro-skeletons also have inhomogeneous Ca contents of 37.5–38.6 wt%, and we considered whether this might contribute to the observed  $\delta^{18}\text{O}$  variation. However, the correlation between SIMS  $\delta^{18}\text{O}$  values and EPMA Ca contents of coral skeletons from close sampling locations is insignificant (Fig. 8), so Ca content variability cannot explain the  $\delta^{18}\text{O}$  heterogeneity observed here. Furthermore,  $\delta^{18}\text{O}$  values of tropical coral obtained by the conventional method were previously considered

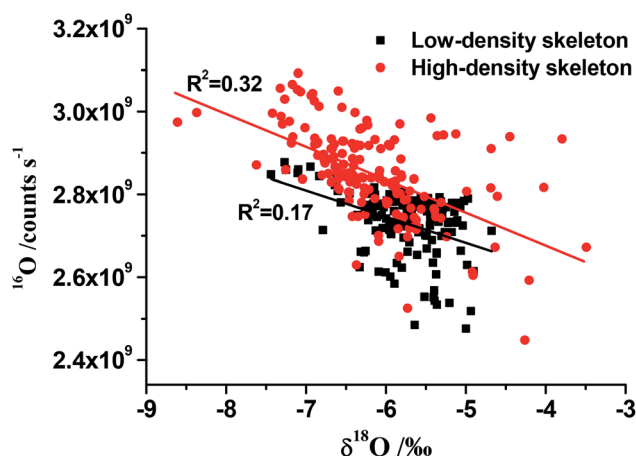


Fig. 7 Relationship between  $^{16}\text{O}$  count rate and  $\delta^{18}\text{O}$  value for individual SIMS analyses along the transect of low- and high-density coral skeletons.

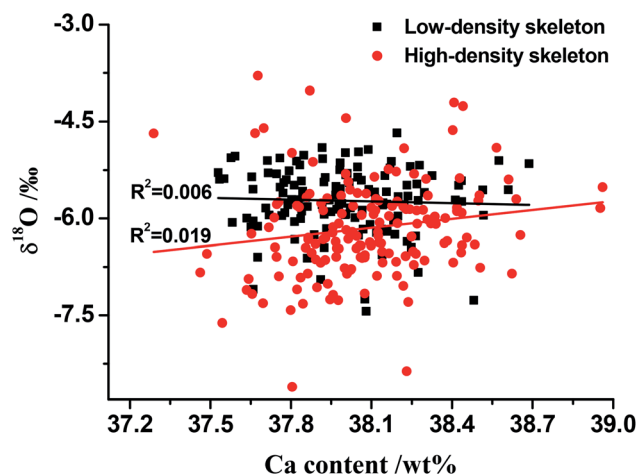


Fig. 8 Relationship between Ca content and  $\delta^{18}\text{O}$  value analyses along the transect of low- and high-density coral skeletons.

to reflect sea surface temperature (SST) and seawater  $\delta^{18}\text{O}$  composition,<sup>6,51,52</sup> although low- and high-density skeleton  $\delta^{18}\text{O}$  values ranged from  $-4.68\text{‰}$  to  $-7.44\text{‰}$  and from  $-3.49\text{‰}$  to  $-8.61\text{‰}$ , respectively. Such short-term heterogeneity is too large to be generated by variations in SST and/or seawater  $\delta^{18}\text{O}$  values at the study site. Local mean SST typically varies by  $\leq 6$  °C annually,<sup>8,53</sup> which could produce a shift in coral  $\delta^{18}\text{O}$  values of  $\sim 0.85\text{‰}$  based on the  $\delta^{18}\text{O}$ -SST regression relationship,  $\delta^{18}\text{O} = -0.142 \times \text{SST} - 1.567$ , obtained by Wang *et al.*<sup>8</sup> from monthly records of the same coral. Likewise, the local annual salinity ranges is  $\sim 33.48$ – $33.94$  p. s. u.,<sup>8,54</sup> corresponding to an additional variations in seawater  $\delta^{18}\text{O}$  values of only  $0.12\text{‰}$  based on the  $\delta^{18}\text{O}$ /salinity relationship of about  $0.27\text{‰}$  per p. s. u.<sup>55,56</sup> The effect of environmental variations on coral  $\delta^{18}\text{O}$  values is thus much smaller than the measured micro-skeleton variability, which is also beyond the range of isotopic equilibrium values for inorganic aragonite ( $-1.78\text{‰}$  to  $-2.87\text{‰}$ ; calculated with environmental parameters at the sampling location).<sup>1</sup> Such



heterogeneity in micro-skeleton oxygen isotopic composition therefore indicates that it is not driven directly by environmental (temperature and salinity) factors, but is controlled mainly by other processes such as vital effects, as supported by the observation by Juillet-Leclerc *et al.*<sup>9</sup> of  $\delta^{18}\text{O}$  variations of up to  $\sim 3\text{‰}$  in SIMS analyses of *Acropora* coral cultured under constant temperature and seawater isotopic composition. It follows that  $\delta^{18}\text{O}$  values derived from microstructures likely do not indicate conditions prevailing in seawater (as suggested by conventional analyses), but rather provide information about the internal conditions created by biological activity at the specific locations in the skeleton and at the time of precipitation.<sup>9,11</sup>

Coral skeletal  $\delta^{18}\text{O}$  micro-heterogeneity may be primarily affected by the pH of the calcifying fluid in which the skeletons precipitate,<sup>11,34</sup> possibly inducing significant variations in proportions of dissolved carbonate species ( $\text{H}_2\text{CO}_3$ ,  $\text{HCO}_3^-$ , and  $\text{CO}_3^{2-}$ ) whose  $\delta^{18}\text{O}$  values at equilibrium with seawater are distinctly different.<sup>34,44,57</sup> Microsensor measurement in corals by Al-Horani *et al.*<sup>58</sup> have shown that the pH of the calcifying fluid ranges from 8.13 to 9.29. The regulation of pH is controlled by activity of Ca-ATPase, which predominantly determines the pH of calcifying fluid through exchange with  $\text{Ca}^{2+}$ .<sup>59,60</sup> The metabolisms of coral and symbiotic zooxanthellae also have extra influences.<sup>34,61</sup> Both bio-processes may induce variation of calcifying fluid pH and thus the skeletal oxygen isotopic composition. The residence time of dissolved carbonate species at the calcification site may also contribute to the  $\delta^{18}\text{O}$  variability, as it may reflect the degree of equilibrium with surrounding water.<sup>34,44</sup> Coral calcification may thus be regarded as a biological process mediated by enzymes and membrane exchange processes, implying that local calcification conditions may be strongly regulated by cell activity or coral tissues near the mineralization process.<sup>21</sup>

## 5. Conclusion

A new aragonite standard for *in situ* oxygen isotopic analysis by SIMS was developed with  $\sim 0.3\text{‰}$  multi-measurement reproducibility. SIMS aragonite IMF cause  $\delta^{18}\text{O}$  values increase linearly by  $\sim 3.4\text{‰}$  with increasing Ca content. The use of multiple aragonite reference materials that compositionally bracket the unknown sample is therefore highly recommended to accurately correct the oxygen isotopic measurements. The variability of oxygen isotopic composition at the micrometer scales in coral skeletons exceeds by far the range expected for coral grown in a known environment, which may indicate a path toward understanding the complex biological processes associated with coral growth.

## Conflicts of interest

There are no conflicts to declare.

## Acknowledgements

The English of the manuscript was improved by Stallard Scientific Editing. This work was supported by the National

Natural Sciences Foundation of China (41803010 and 42021002), the GIGCAS 135 Project (135PY201605), the Guangzhou Institute of Geochemistry (TGC201804), the State Key Laboratory of Isotope Geochemistry (SKLaBIG-JY-19-04) and the State Key Laboratory of Loess and Quaternary Geology, Institute of Earth Environment, CAS (SKLLQG1932). This is contribution No. IS-3028 from GIGCAS.

## References

- 1 S.-T. Kim, J. R. O'Neil, C. Hillaire-Marcel and A. Mucci, Oxygen isotope fractionation between synthetic aragonite and water: Influence of temperature and  $\text{Mg}^{2+}$  concentration, *Geochim. Cosmochim. Acta*, 2007, **71**, 4704–4715.
- 2 J. M. Eiler, J. W. Valley, C. M. Graham and J. Fournelle, Two populations of carbonate in ALH84001: geochemical evidence for discrimination and genesis, *Geochim. Cosmochim. Acta*, 2002, **66**, 1285–1303.
- 3 T. Watanabe, M. K. Gagan, T. Corregge, H. Scott-Gagan, J. Cowley and W. S. Hantoro, Oxygen isotope systematics in *Diploastrea heliopora*: new coral archive of tropical paleoclimate, *Geochim. Cosmochim. Acta*, 2003, **67**, 1349–1358.
- 4 C. Rollion-Bard, D. Mangin and M. Champenois, Development and Application of Oxygen and Carbon Isotopic Measurements of Biogenic Carbonates by Ion Microprobe, *Geostand. Geoanal. Res.*, 2007, **31**, 39–50.
- 5 T. Chen, K. Yu, J. Zhao, H. Yan, Y. Song, Y. Feng and T. Chen, Testing coral paleothermometers (B/Ca, Mg/Ca, Sr/Ca, U/Ca and  $\delta^{18}\text{O}$ ) under impacts of large riverine runoff, *Acta Oceanol. Sin.*, 2015, **34**, 20–26.
- 6 A. Juillet-Leclerc and G. Schmidt, A calibration of the oxygen isotope paleothermometer of coral aragonite from Porites, *Geophys. Res. Lett.*, 2001, **28**, 4135–4138.
- 7 T. Mitsuguchi, Evaluation of the effects of microscale chemical and isotopic heterogeneity of coral skeleton on conventional Sr/Ca and  $\delta^{18}\text{O}$  paleothermometers, *J. Earth Syst. Sci.*, 2013, **122**, 1335–1340.
- 8 X. Wang, W. Deng, X. Liu, G. Wei, X. Chen, J.-x. Zhao, G. Cai and T. Zeng, Super instrumental El Niño events recorded by a Porites coral from the South China Sea, *Coral Reefs*, 2018, **37**, 295–308.
- 9 A. Juillet-Leclerc, S. Reynaud, C. Rollion-Bard, J. P. Cuif, Y. Dauphin, D. Blamart, C. Ferrier-Pagès and D. Allemand, Oxygen isotopic signature of the skeletal microstructures in cultured corals: Identification of vital effects, *Geochim. Cosmochim. Acta*, 2009, **73**, 5320–5332.
- 10 C. Rollion-Bard, D. Blamart, J.-P. Cuif and A. Juillet-Leclerc, Microanalysis of C and O isotopes of azooxanthellate and zooxanthellate corals by ion microprobe, *Coral Reefs*, 2003, **22**, 405–415.
- 11 C. Rollion-Bard and D. Blamart, SIMS method and examples of applications in coral biomineralization, ed Gower L. B. and DiMasi E., in *Biomineralization Handbook. Characterization of Biominerals and Biomimetic Materials*, Taylor & Francis, United Kingdom, 2014, pp. 249–261.

- 12 C. L. Pederson, V. Mavromatis, M. Dietzel, C. Rollion-Bard, S. F. M. Breitenbach, D. Yu, G. Nehrke and A. Immenhauser, Variation in the diagenetic response of aragonite archives to hydrothermal alteration, *Sediment. Geol.*, 2020, **406**, 105716.
- 13 A. Kahal, A. El-Sorogy, H. Alfaifi, S. Almadani and O. Kassem, Biofacies and diagenetic alterations of the Pleistocene coral reefs, northwest Red Sea coast, Saudi Arabia, *Geol. J.*, 2020, **55**, 1380–1390.
- 14 J. Michal, B. Blazej, L. C. Matthias, J. Emilia, J. Michael and B. Zdzislaw, Stable Isotope Signatures of Middle Palaeozoic Ahermatypic Rugose Corals - Deciphering Secondary Alteration, Vital Fractionation Effects, and Palaeoecological Implications, *PLoS One*, 2015, **10**, DOI: 10.1371/journal.pone.0136289.
- 15 N. Allison, A. A. Finch, J. M. Webster and D. A. Clague, Palaeoenvironmental records from fossil corals: The effects of submarine diagenesis on temperature and climate estimates, *Geochim. Cosmochim. Acta*, 2007, **71**, 4693–4703.
- 16 H. R. Sayani, K. M. Cobb, A. L. Cohen, W. C. Elliott, I. S. Nurhati, R. B. Dunbar, K. A. Rose and L. K. Zaunbrecher, Effects of diagenesis on paleoclimate reconstructions from modern and young fossil corals, *Geochim. Cosmochim. Acta*, 2011, **75**, 6361–6373.
- 17 Q. Yu, L. F. Li, E. Y. Zhu, W. Hang, J. A. He and B. L. Huang, Analysis of solids with different matrices by buffer-gas-assisted laser ionization orthogonal time-of-flight mass spectrometry, *J. Anal. At. Spectrom.*, 2010, **25**, 1155–1158.
- 18 H. Yan, C. Liu, Z. An, W. Yang, Y. Yang, P. Huang, S. Qiu, P. Zhou, N. Zhao, H. Fei, X. Ma, G. Shi, J. Dodson, J. Hao, K. Yu, G. Wei, Y. Yang, Z. Jin and W. Zhou, Extreme weather events recorded by daily to hourly resolution biogeochemical proxies of marine giant clam shells, *Proc. Natl. Acad. Sci. U. S. A.*, 2020, **117**, 7038–7043.
- 19 J. M. Eiler, C. Graham and J. W. Valley, SIMS analysis of oxygen isotopes: matrix effects in complex minerals and glasses, *Chem. Geol.*, 1997, **138**, 221–244.
- 20 M. G. Śliwiński, K. Kitajima, R. Kozdon, M. J. Spicuzza, J. H. Fournelle, A. Denny and J. W. Valley, Secondary Ion Mass Spectrometry Bias on Isotope Ratios in Dolomite–Ankerite, Part I:  $\delta^{18}\text{O}$  Matrix Effects, *Geostand. Geoanal. Res.*, 2016, **40**, 157–172.
- 21 J. P. Jones, J. P. Carricart-Ganivet, R. Iglesias Prieto, S. Enriquez, M. Ackerson and R. I. Gabitov, Microstructural variation in oxygen isotopes and elemental calcium ratios in the coral skeleton of *Orbicella annularis*, *Chem. Geol.*, 2015, **419**, 192–199.
- 22 C. Fabrega, D. Parcerisa, J. Rossell, A. Gurenko and C. Franke, Predicting instrumental mass fractionation (IMF) of stable isotope SIMS analyses by response surface methodology (RSM), *J. Anal. At. Spectrom.*, 2017, **32**, 731–748.
- 23 N. Shimizu and S. Hart, Isotope fractionation in secondary ion mass spectrometry, *J. Appl. Phys.*, 1982, **53**, 1303–1311.
- 24 D. Vielzeuf, M. Champenois, J. W. Valley, F. Brunet and J. L. Devidal, SIMS analyses of oxygen isotopes: Matrix effects in Fe–Mg–Ca garnets, *Chem. Geol.*, 2005, **223**, 208–226.
- 25 C. Rollion-Bard, D. Blamart, J.-P. Cuif and Y. Dauphin, In situ measurements of oxygen isotopic composition in deep-sea coral, *Lophelia pertusa*: Re-examination of the current geochemical models of biomineralization, *Geochim. Cosmochim. Acta*, 2010, **74**, 1338–1349.
- 26 M. Fayek, T. M. Harrison, M. Grove, K. D. Mckeegan, C. D. Coath and J. R. Boles, In situ Stable Isotopic Evidence for Protracted and Complex Carbonate Cementation in a Petroleum Reservoir, North Coles Levee, San Joaquin Basin, California, U.S.A, *J. Sediment. Res.*, 2001, **71**, 444–458.
- 27 C. Rollion-Bard and J. Marin-Carbonne, Determination of SIMS matrix effects on oxygen isotopic compositions in carbonates, *J. Anal. At. Spectrom.*, 2011, **26**, 1285–1289.
- 28 P. T. Spooner, T. Chen, L. F. Robinson and C. D. Coath, Rapid uranium-series age screening of carbonates by laser ablation mass spectrometry, *Quat. Geochronol.*, 2016, **31**, 28–39.
- 29 N. Kampman, M. Bickle, J. Becker, N. Assayag and H. Chapman, Feldspar dissolution kinetics and Gibbs free energy dependence in a  $\text{CO}_2$ -enriched groundwater system, Green River, Utah, *Earth Planet. Sci. Lett.*, 2009, **284**, 473–488.
- 30 N. Kampman, N. M. Burnside, Z. K. Shipton, H. J. Chapman, J. A. Nicholl, R. M. Ellam and M. J. Bickle, Pulses of carbon dioxide emissions from intracrustal faults following climatic warming, *Nat. Geosci.*, 2012, **5**, 352–358.
- 31 J.-Q. Zou, G.-J. Wei, W.-F. Deng, X.-F. Chen, Q. Yang and X.-P. Xia, Analysis of oxygen isotopic compositions of coral using Secondary Ion Mass Spectrometry, *Geochimica*, 2018, **47**, 306–312.
- 32 S. Von Euw, Q. Zhang, V. Manichev, N. Murali, J. Gross, L. C. Feldman, T. Gustafsson, C. Flach, R. Mendelsohn and P. G. Falkowski, Biological control of aragonite formation in stony corals, *Science*, 2017, **356**, 933–938.
- 33 N. Allison and A. A. Finch, Reproducibility of minor and trace element determinations in *Porites* coral skeletons by secondary ion mass spectrometry, *Geochem., Geophys., Geosyst.*, 2009, **10**, DOI: 10.1029/2008GC002239.
- 34 N. Allison and A. A. Finch, The potential origins and palaeoenvironmental implications of high temporal resolution  $\delta^{18}\text{O}$  heterogeneity in coral skeletons, *Geochim. Cosmochim. Acta*, 2010, **74**, 5537–5548.
- 35 M. E. Hartley, T. Thordarson, C. Taylor, J. G. Fitton and EIMF group, Evaluation of the effects of composition on instrumental mass fractionation during SIMS oxygen isotope analyses of glasses, *Chem. Geol.*, 2012, **334**, 312–323.
- 36 C. G. Weinzierl, M. Regelous, K. M. Haase, W. Bach, F. Böhm, D. Garbe-Schönberg, Y. D. Sun, M. M. Joachimski and S. Krumm, Cretaceous seawater and hydrothermal fluid compositions recorded in abiogenic carbonates from the Troodos Ophiolite, Cyprus, *Chem. Geol.*, 2018, **494**, 43–55.
- 37 M. D. L. Pierre, C. Carteret, L. Maschio, E. André, R. Orlando and R. Dovesi, The Raman spectrum of  $\text{CaCO}_3$  polymorphs calcite and aragonite: A combined experimental and computational study, *J. Chem. Phys.*, 2014, **140**, 164509.

- 38 C. Carteret, A. Dandeu, S. Moussaoui, H. Muhr, B. Humbert and E. Plasari, Polymorphism Studied by Lattice Phonon Raman Spectroscopy and Statistical Mixture Analysis Method. Application to Calcium Carbonate Polymorphs during Batch Crystallization, *Cryst. Growth Des.*, 2009, **9**, 807–812.
- 39 A. P. Gajurel, C. France-Lanord, P. Huyghe, C. Guilmette and D. Gurung, C and O isotope compositions of modern freshwater mollusc shells and river waters from the Himalaya and Ganga plain, *Chem. Geol.*, 2006, **233**, 156–183.
- 40 X. Liu, W. Deng and G. Wei, Carbon and oxygen isotopic analyses of calcite in calcite-dolomite mixtures: optimization of selective acid extraction, *Rapid Commun. Mass Spectrom.*, 2019, **33**, 411–418.
- 41 A. Juillet-Leclerc, C. Rollion-Bard, S. Reynaud and C. Ferrier-Pages, A new paradigm for delta O-18 in coral skeleton oxygen isotope fractionation response to biological kinetic effects, *Chem. Geol.*, 2018, **483**, 131–140.
- 42 G. Q. Tang, X. H. Li, Q. L. Li, Y. Liu, X. X. Ling and Q. Z. Yin, Deciphering the physical mechanism of the topography effect for oxygen isotope measurements using a Cameca IMS-1280 SIMS, *J. Anal. At. Spectrom.*, 2015, **30**, 950–956.
- 43 Y. Liu, X.-H. Li, G. Tang, X.-C. Liu, H.-M. Yu and F. Huang, Ultra-high precision silicon isotope micro-analysis using Cameca IMS-1280 SIMS by eliminating the topography effect, *J. Anal. At. Spectrom.*, 2019, **34**, 906–914.
- 44 C. Rollion-Bard, M. Chaussidon and C. France-Lanord, pH control on oxygen isotopic composition of symbiotic corals, *Earth Planet. Sci. Lett.*, 2003, **215**, 275–288.
- 45 A. Vho, D. Rubatto, B. Putlitz and A.-S. Bouvier, New Reference Materials and Assessment of Matrix Effects for SIMS Measurements of Oxygen Isotopes in Garnet, *Geostand. Geoanal. Res.*, 2020, DOI: 10.1111/ggr.12324.
- 46 E. Deloule, C. France-Lanord and F. Albarède, D/H analysis of minerals by ion probe, *Geochem. Soc.*, 1991, **3**, 53–62.
- 47 B. Pokroy, J. P. Quintana, E. a. N. Caspi, A. Berner and E. Zolotoyabko, Anisotropic lattice distortions in biogenic aragonite, *Nat. Mater.*, 2004, **3**, 900–902.
- 48 J. P. Cuif, Y. Y. Dauphin, J. Doucet, M. Salome and J. Susini, XANES mapping of organic sulfate in three scleractinian coral skeletons, *Geochim. Cosmochim. Acta*, 2003, **67**, 75–83.
- 49 E. H. Gladfeiter, Skeletal development in *Acropora cervicornis*: I. Patterns of calcium carbonate accretion in the axial corallite, *Coral Reefs*, 1982, **1**, 45–51.
- 50 A. G. Grottoli, L. J. Rodrigues, K. A. Matthews, J. E. Palardy and O. T. Gibb, Pre-treatment effects on coral skeletal  $\delta^{13}\text{C}$  and  $\delta^{18}\text{O}$ , *Chem. Geol.*, 2005, **221**, 225–242.
- 51 W. Deng, G. Wei, K. Yu and J. X. Zhao, Variations in the timing of the rainy season in the northern South China Sea during the middle to late Holocene, *Paleoceanography*, 2014, **29**, 115–125.
- 52 W. F. Deng, G. J. Wei, X. H. Li, K. F. Yu, J. X. Zhao, W. D. Sun and Y. Liu, Paleoprecipitation record from coral Sr/Ca and  $\delta^{18}\text{O}$  during the mid Holocene in the northern South China Sea, *Holocene*, 2009, **19**, 811–821.
- 53 B. Huang, V. F. Banzon, E. Freeman, J. Lawrimore, W. Liu, T. C. Peterson, T. M. Smith, P. W. Thorne, S. D. Woodruff and H.-M. Zhang, Extended Reconstructed Sea Surface Temperature Version 4 (ERSST.v4). Part I: Upgrades and Intercomparisons, *J. Clim.*, 2015, **28**, 911–930.
- 54 S. A. Good, M. J. Martin and N. A. Rayner, EN4: Quality controlled ocean temperature and salinity profiles and monthly objective analyses with uncertainty estimates, *J. Geophys. Res.: Oceans*, 2013, **118**, 6704–6716.
- 55 M. K. Gagan, L. K. Ayliffe, J. W. Beck, J. E. Cole, E. R. M. Druffel, R. B. Dunbar and D. P. Schrag, New views of tropical paleoclimates from corals, *Quat. Sci. Rev.*, 2000, **19**, 45–64.
- 56 R. G. Fairbanks, M. N. Evans, J. L. Rubenstone, R. A. Mortlock, K. Broad, M. D. Moore and C. D. Charles, Evaluating climate indices and their geochemical proxies measured in corals, *Coral Reefs*, 1997, **16**, S93–S100.
- 57 E. Usdowski, J. Michaelus, M. Böttcher and J. Hoefs, Factors for the oxygen isotope equilibrium fractionation between aqueous and gaseous carbon dioxide, carbonic acid, bicarbonate, carbonate, and water (19°C), *Z. Phys. Chem.*, 1991, **170**, 237–249.
- 58 F. Al-Horani, S. Al-Moghrabi and D. De Beer, The mechanism of calcification and its relation to photosynthesis and respiration in the scleractinian coral *Galaxea fascicularis*, *Mar. Biol.*, 2003, **142**, 419–426.
- 59 J. F. Adkins, E. A. Boyle, W. B. Curry and A. Lutringer, Stable isotopes in deep-sea corals and a new mechanism for “vital effects”, *Geochim. Cosmochim. Acta*, 2003, **67**, 1129–1143.
- 60 C. Rollion-Bard, M. Chaussidon and C. France-Lanord, Biological control of internal pH in scleractinian corals: Implications on paleo-pH and paleo-temperature reconstructions, *C. R. Geosci.*, 2011, **343**, 397–405.
- 61 A. Juillet-Leclerc, S. Reynaud, D. Dissard, G. Tisserand and C. Ferrier-Pages, Light is an active contributor to the vital effects of coral skeleton proxies, *Geochim. Cosmochim. Acta*, 2014, **140**, 671–690.